frontiers | Frontiers in Earth Science

TYPE Original Research
PUBLISHED 10 August 2022
DOI 10.3389/feart.2022.895884

OPEN ACCESS

EDITED BY
Xiaoyan Zhao,
Southwest Jiaotong University, China

REVIEWED BY
Zhao Liu,
Hebei GEO University, China
Yanyan Li,
Chinese Academy of Geological Sciences (CAGS), China

*CORRESPONDENCE
Mo Xu,
xm@cdut.edu.cn

SPECIALTY SECTION
This article was submitted to Geohazards and Georisks, a section of the journal Frontiers in Earth Science

RECEIVED 14 March 2022
ACCEPTED 11 July 2022
PUBLISHED 10 August 2022

CITATION
Zhang W, Xu M and Wu S (2022), Study on the genetic mechanism of high-temperature geothermal system and its engineering impact in the Woka graben, Tibet.
Front. Earth Sci. 10:895884.
doi: 10.3389/feart.2022.895884

Study on the genetic mechanism of high-temperature geothermal system and its engineering impact in the Woka graben, Tibet

Wen Zhang[1,2], Mo Xu[1]* and Sen Wu[3]

[1]Chengdu University of Technology, Chengdu, Sichuan, China, [2]Institute of Exploration Technology, Chinese Academy of Geological Sciences, Chengdu, Sichuan, China, [3]Sichuan Institute of Geological Engineering Investigation Group Co. Ltd., Chengdu, Sichuan, China

The geothermal resource has become the significant constitution of renewable and clean energies in the world. This study focuses on the genetic mechanism of a high-temperature geothermal system and its engineering impact in the Woka graben, southern Tibet, via hydrochemical and isotopic analyses. The hydrochemical types are mainly SO_4-Na type, SO_4-Cl-Na type, and HCO_3-SO_4-Na type. Geothermal water is characterized as medium to alkaline affinity with low total dissolved solids. D-O isotopes indicate that geothermal water is recharged by atmospheric precipitation at the elevation of 5193–5247 m. Na-K-Mg equilibrium diagram shows partial equilibrium or mixed water, and the proportion of cold water mixing is 73–83%. The temperature ranges of shallow and deep geothermal reservoirs are from 96.85°C to 119.57°C and from 120°C to 200°C, respectively. Geothermal water is heated by melting crust and controlled by deep faults. For major construction projects in the Woka graben, detailed investigation and demonstration should be conducted to avoid the geothermal water channel as much as possible, or to divert the geothermal water and reasonably arrange the construction sequence to overcome the problem.

KEYWORDS

formation mechanism, high-temperature geothermal system, hydrochemical characteristics, D-O-C isotopes, engineering influence

Introduction

Among the more than 3,000 hydrothermal activity areas identified in China, 677 are occurring in Tibet (Liao, 2018; Wang et al., 2018; Zhang and Hu, 2018). In addition, 342 geothermal manifestations are available for exploration, with the vast majority having a temperature of more than 80°C. Geothermal resource in Tibet is characterized by high-temperature, various types, and extensive distribution (Guo, 2012; Kong et al., 2014). The distribution of geothermal resources in Tibet is strictly controlled by active faults and is closely related to the regional geothermal heat flow background (Jiang et al., 2018; Tan et al., 2018). Taking the high-temperature vapor geothermal manifestations in southern Tibetan as an example, numerous active tectonic belts have developed in the N-S direction and consist of a series of uplift

zones and fracture zones along the Himalayan arc tectonic belt. Afterward, a series of Quaternary graben basins were formed, in which strong modern hydrothermal activity has developed, e.g., the Langjiu, Kawu, Yangbajing, and Gudui geothermal fields (Zhang et al., 2015; Wang et al., 2016).

The Cona–Woka rift valley belt is the easternmost side of the Tibetan rift valley belt near the north–south fracture belt, by the Woka, Qiongduojiang, and Cona grabens. The graben is enriched in geothermal resources, where the second largest geothermal manifestation (Gudui geothermal field) in Tibet is distributed. The Woka geothermal manifestation is located in the Woka graben in the northern section of the Cona–Woka rift valley. Along the Zengjiuqu River valley and slope, geothermal manifestation with a length of 3 km and temperature of 43°C–68.2°C is developed, belonging to the low- to medium-temperature geothermal system. Previous studies focused on the hydrochemical characteristics and genetic mechanism of geothermal waters in Tibet (Elenga et al., 2021; Li et al., 2021; Tian et al., 2021; Wang et al., 2021; Klemperer et al., 2022; Wang et al., 2022). However, the studies on the genesis mode of the Woka geothermal springs are lacking. The geothermal reservoir and heat source are still unclear, making it difficult to evaluate the prospecting potential. So far, the Woka geothermal springs have been utilized for the bathing function. Therefore, research on the genetic mechanism of the Woka geothermal system can provide scientific guidance for the assessment of geothermal resource potential in the Woka graben and other areas in southern Tibet.

In this study, the hydrogeochemical characteristics, reservoir temperature, and subsurface cold water mixing ratio of geothermal springs in the Woka geothermal system are comprehensively studied using hydrochemical and isotopic data. Afterward, the conceptual model of a medium- to high-temperature geothermal system in the Woka geothermal zone is established. At last, the engineering significance of the geothermal system is investigated.

Study area

The study area is located in Sangri Township and Lobsa Township, 40 km away from Sangri County, Tibet. The study area has an alpine valley landform, steep bank slope, terrain slope of 30°–50°, and a height difference of 1000–1500 m. The climate in the area belongs to the plateau temperate monsoon semihumid climate zone, with an annual average temperature of 6.4°C–8.2°C and annual average precipitation of 500–600 mm, mainly concentrated from May to September, accounting for more than 89% of the annual rainfall. Rainfall has the characteristics of large annual variation and concentrated rainfall periods.

The Woka graben basin is located in the Himalayas terrane (Zhang et al., 2019a, 2022; Cao et al., 2019). The geothermal water system in the Woka graben basin is composed of the many geothermal springs distributed along the Zengjiuqu River valley in Woka graben basin, with 22 existing geothermal springs and a total flow rate of more than 20 L/s (Table 1). According to the characteristics of the underground geothermal water outcropping and the current situation of development and utilization, it can be divided into Kanai, Woka, Cuoba, and Lobosha geothermal springs. The upper part is light yellow subsandy or gravelly subsandy soil, and the lower part is mixed-colored pebbles, drift stones, and muddy pebbles. The Cretaceous–Paleocene black mica diorite ($\eta\gamma\beta K_2$), granodiorite ($\gamma\delta K_1$), quartz diorite (δoK_1), *etc*. are distributed along the watershed; the Middle to Lower Jurassic Yerba Formation ($J_{1-2}y$) is exposed along the watershed, divided into three lithological sections: the first section is characterized by volcanic breccia and volcanic agglomerate; the second section is dominated by medium-acid andesite, andesite, rhyolite, and crystalline clastic tuff; and the third section is composed of sunken tuff, metamorphic sandstone, and siltstone. The geothermal geological background of the Woka graben is shown in Figure 1.

Woka basin is located in southern Tibet near the N-S development rift valley—the northern section of the Cuona—Woka rift valley, for regional extension and deformation, and the formation of the Quaternary activity is an obvious graben-type fracture basin (Cao et al., 2020; Cao et al., 2021). The total length of the rift basin is approximately 50 km, north of the Jinzhu township area, the southern end of the Luobusha chromite. Region-wise, the southern end of the Woka graben is bounded by the south-trending rebound fault zone, Yarlung Tsangpo River suture tectonic zone, and the north-trending Xela-Riduo-Palo fault in the northern section, which is interrupted by the near E-S trending development of the Mocun ductile fault and some pot faults.

The main boundary fault zone controlling the development of the Woka basin is the NNE-trending, west-trending, 50- to 60-km-long orthotropic fault on the eastern margin of the basin (Zhang et al., 2019b). In addition, there are ultra-low-resistance areas with a resistivity of less than 50 Ω m along the Zengjiuqu River valley based on several high-density physical profiles. Meanwhile, seismic activity is frequent within the Woka graben basin, and the results of fracture activity rate estimation indicate the vertical activity rate of this fault zone since MIS six ranges from 0.4 to 0.9 mm/a. Under the effect of long-term seismic activity, a network of tectonic fissures has been formed in the Woka graben basin that crosses east–west and north–south directions, providing storage space and runoff channels for the development of the underground geothermal water system in the Woka graben basin.

TABLE 1 Exposure characteristics of geothermal springs.

Name	Flow/L·s^{-1}	T/°C	TDS/mg L^{-1}	Location
Kanai geothermal spring	>1	53.3	744	Right bank of the Zengjiuqu I class terrace
Woka geothermal spring	>10	25–50.5	345–403	Right slope of Zengjiuqu
Cuoba geothermal spring	1.5	36.25	285.9	Right bank of the Zengjiuqu I class terrace
Luobusha geothermal spring	1.7	57.77	8642.95	Right bank of the Yarlung Tsangpo River
Amaka geothermal spring	3.86	35.7	404	Right bank of the Zengjiuqu I class terrace
Woka hekou spring	3	13.3	171	North bank of the Yajiang River
Zhumosha geothermal spring	—	55–75.5	—	Right bank of the Yarlung Tsangpo River

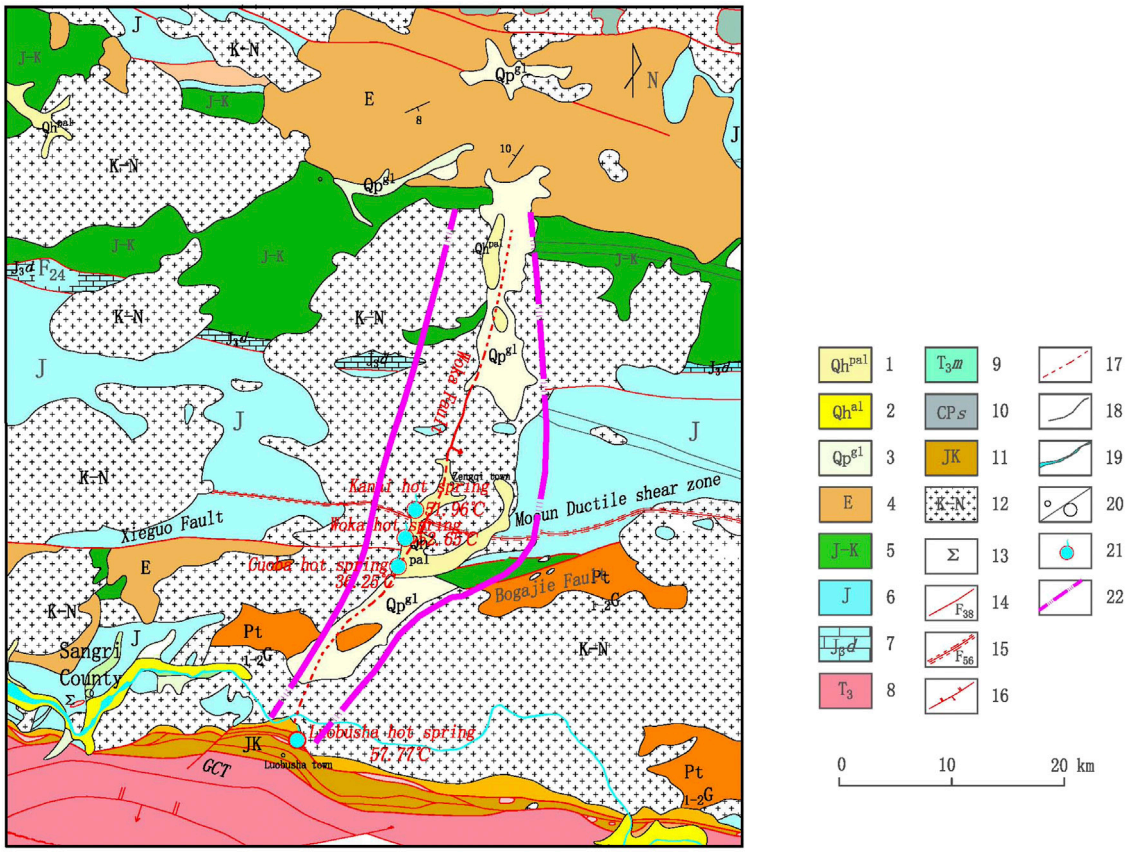

FIGURE 1
Geological background map of Oiga Graben basin. 1-Holocene alluvial deposits; 2-Holocene alluvium; 3-Pleistocene glacial deposits; 4-Paleogene volcanic rocks; 5-Late Jurassic Cretaceous and Cretaceous; 6-Sedimentary assemblage of Jurassic volcanic and continental clastic rocks; 7-Duodigou formation limestone; 8-Late Triassic Century; 9-Mailonggang formation; 10-Songduo group; 11-Jurassic-Cretaceous melange; 12-Cretaceous-Neogene intrusive rocks; 13-Ultrabasic block; 14-Fault and number; 15-Ductile shear zone and number; 16-Reverse fault; 17-Inferred fault; 18-Geological boundary; 19-River system; 20-Town/City; 21-Hot spring; 22-Range of fault graben basin.

Sampling and methodology

In this study, four geothermal water samples were collected in January 2020 for the experiments of hydrochemistry, δ^2H, $\delta^{18}O$, and $\delta^{13}C$. pH, total dissolved solids (TDS), and flow were measured in the field using a portable WTW device. The HCO_3^- content was *in situ* constraint by Gran titration. K^+, Na^+, Ca^{2+}, and Mg^{2+} were determined via inductively coupled plasma-optical emission spectrometry, and Cl^- and SO_4^{2-} were measured via ion chromatography (Dionex ICS-1100) in the State Key Laboratory

TABLE 2 Hydrochemical and D-O-C isotopic results of geothermal springs.

Parameter		Kanai geothermal spring	Woka geothermal spring	Cuoba geothermal spring	Luobusha geothermal spring
T/°C		51.96	52.65	36.25	57.77
pH		8.25	8.25	7.95	6.71
TDS/(mg/L)		440.51	398.43	285.90	8642.95
Cation/(mg/L)	K^+	1.90	1.97	1.48	343
	Na^+	111	106	63.9	1472
	Mg^{2+}	0.026	0.088	0.44	7.85
	Ca^{2+}	5.24	7.69	12.2	80.6
Anion/(mg/L)	HCO_3^-	31	43	37	214
	SO_4^{2-}	147	137	94.4	120
	Cl^-	42.5	52.7	31.8	4060
H_2SiO_3/(mg/L)		74.9	62.4	43.3	312
δ^2H/‰		−156.3	−154.8	−150.8	−129.5
$\delta^{18}O$/‰		−19.86	−19.71	−19.46	−11.96
d=δD-8δ^{18}O		2.58	2.88	4.88	−33.82
$\delta^{13}C$/‰		−6.1	−6.49	−5.41	−3.45
Hydrochemical type		SO_4-Na	Cl·SO_4-Na	HCO_3·SO_4-Na	Cl-Na

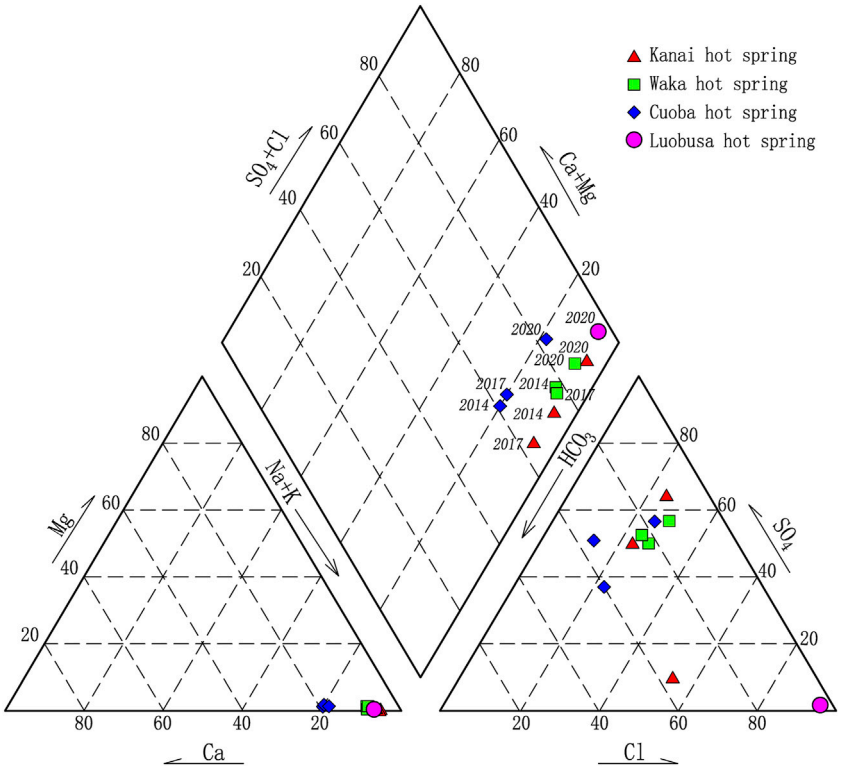

FIGURE 2
Piper diagram of geothermal waters.

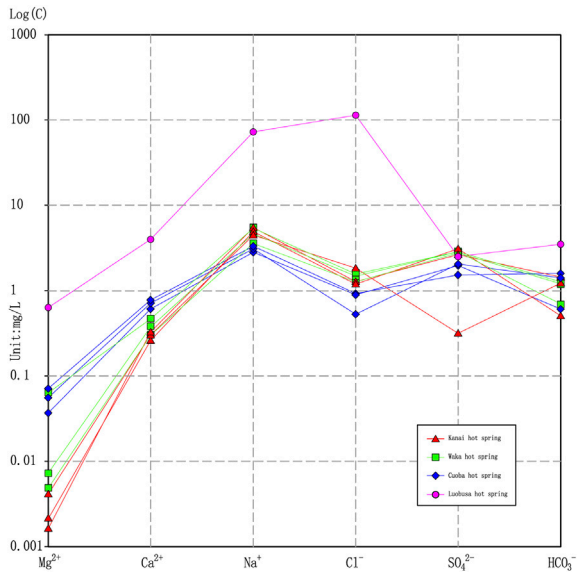

FIGURE 3
Schöeller diagram of geothermal waters.

of Geohazard Prevention and Geoenvironment Protection, Chengdu University of Technology. The charge balance was lower than ±10%. δD and $\delta^{18}O$ were analyzed using a mass spectrometer (MAT253), and $\delta^{13}C$ was measured via stable isotope ratio mass spectrometry (Delta Plus XP) at the Institute of Karst Geology, Chinese Academy of Geological Science.

Results and discussion

Water–rock interaction by hydrochemical characteristics

Table 2 shows that the water chemistry of geothermal water in the Woka geothermal area is dominated by Na^+, Ca^{2+}, and K^+ in cations and SO_4^{2-} and Cl^- in anions, followed by HCO_3^-. The pH values and total dissolved solid concentrations are 7.95–8.25 and 285.90–440.51 mg/L, respectively. Geothermal waters belong to medium–high alkaline water. The hydrochemistry types are mainly SO_4-Na type, Cl-SO_4-Na type, and HCO_3-SO_4-Na type.

The hydrochemical characteristics of geothermal water and bedrock fracture cold water in the fault rift basin are very different (Figure 2). The geothermal waters are enriched in H_2S but poor in CO_2. Their hydrochemical type is influenced by H_2S, and there are more complex hydrochemical types such as SO_4 type, SO_4-Cl type, and HCO_3-SO_4 type, consistent with the Riduo geothermal spring and Gudui geothermal field in the fault rift zone. The hydrochemical type of the Luobusa geothermal spring is different from that of geothermal waters in the Woka rift, indicating that they do not belong to the same geothermal system.

As shown in the Schoeller diagram (Figure 3), all ions in the geothermal water have regular variations, revealing that the source and formation pattern of geothermal water in the basin have similar characteristics. In addition, the geothermal waters have high SO_4^{2-} contents, consistent with the strong sulfur smell of the geothermal water outcrop, as typified by the Woka geothermal spring. The source of SO_4^{2-} in geothermal water is mainly from geothermal water dissolution filtration of sulfate rocks, and a small part is H_2S carried by deep fluids. Therefore, the higher SO_4^{2-} contents in the geothermal water of Woka mainly come from the strong dissolution filtration of volcanic clastic rocks such as andesitic and rhyolitic lava dominated by the Yeba Formation strata. The saturation indices of geothermal water calculated using Phreeqc software are mostly lower than zero. The results show that most minerals, except for chalcedony and quartz, are unsaturated (Table 3), reflecting the short runoff pathway and weak water–rock reaction.

Four geothermal water samples were taken for $\delta^{13}C$ analysis. The $\delta^{13}C$ values of geothermal spring water are −6.49‰ to −3.45‰: the $\delta^{13}C$ value of Kanai geothermal spring is −6.1‰, the $\delta^{13}C$ value of Woka geothermal spring is −6.49‰, the $\delta^{13}C$ value of Misbah geothermal spring is −5.41‰, and the $\delta^{13}C$ value of Lobsa geothermal spring is −3.45‰ (Figure 4). Previous studies showed that the $\delta^{13}C$ value of upper mantle material source is −8‰ to −4‰, the $\delta^{13}C$ value of carbonate metamorphic source is −2‰ to +2‰, and the $\delta^{13}C$ value of carbonate metamorphic source is −2‰ to +2‰. Therefore, it is presumed that mantle-sourced CO_2 from deep faults was involved in the formation of geothermal waters in the study area.

Recharge source implied by D-O isotopes

Four geothermal water samples were selected for the analysis of hydrogen and oxygen isotopes. The results show that the δ^2H values range from −150.8‰ to −156.3‰ and the $\delta^{18}O$ values range from −19.46‰ to −19.86‰. In Figure 5, all samples are distributed near the global atmospheric precipitation equation line, indicating that the source is recharged by atmospheric precipitation and less infiltration of snow-melting water. The deuterium excess parameter (d) is similar between the geothermal spring and the cold spring, indicating that there is no obvious oxygen drift in the geothermal water. The result reveals the characteristics of atmospheric precipitation recharge and shallow circulation in the geothermal water system of the Woka rift. The deuterium excess parameter d of the Luobusa geothermal spring is −33.82, which shows significant oxygen

TABLE 3 Saturation indices of geothermal springs.

Mineral phase	Chemical content	Kanai spring	Woka spring	Cuoba spring	Luobusha spring
Anhydrite	$CaSO_4$	−2.48	−2.34	−2.46	−1.93
Aragonite	$CaCO_3$	−0.90	−0.55	−0.85	−0.56
Calcite	$CaCO_3$	−0.77	−0.43	−0.71	−0.43
Chalcedony	SiO_2	0.33	0.25	0.28	0.94
Quartz	SiO_2	−0.42	−0.51	−0.53	0.20
Chrysotile	$Mg_3Si_2O_5(OH)_4$	−4.23	−2.71	−4.29	−4.64
Dolomite	$CaMg(CO_3)_2$	−3.39	−2.32	−2.43	−1.36
Gypsum	$CaSO_4{:}2H_2O$	−2.46	−2.32	−2.27	−1.96
Halite	NaCl	−6.91	−6.83	−7.03	−3.96
Sylvite	KCl	−8.34	−8.24	−8.50	−4.29
O_2(g)	O_2	−25.85	−25.66	−31.72	−30.40
CO_2(g)	CO_2	−3.68	−3.51	−3.34	−1.25

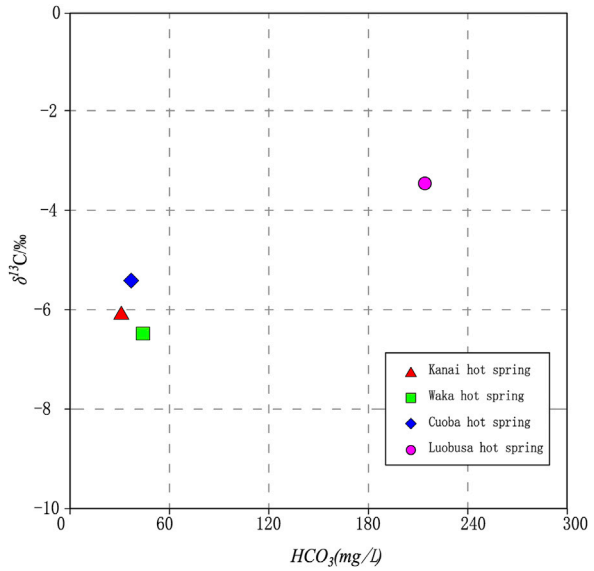

FIGURE 4
$\delta^{13}C$-HCO_3 plot of geothermal waters.

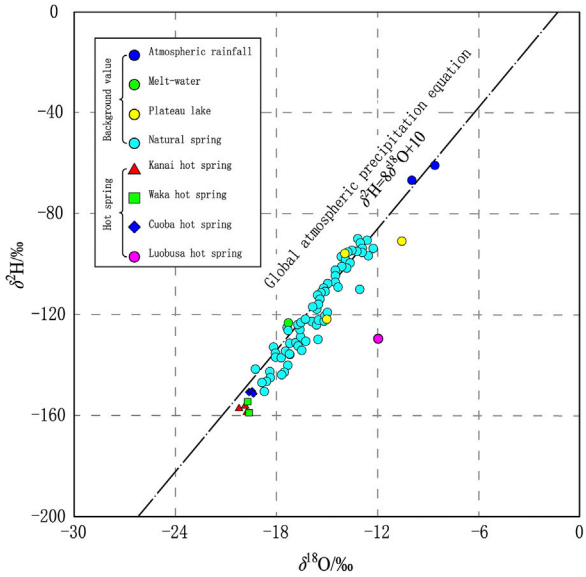

FIGURE 5
δ^2H-$\delta^{18}O$ plot of geothermal waters.

drift, further supporting that it belongs to a different geothermal system from the Woka graben, with deep circulation recharge characteristics.

The isotopic composition of atmospheric precipitation has an elevation effect, and the recharge elevation of geothermal springs can be calculated using $\delta^{18}O$ isotopic values based on this feature (Zhang et al., 2018). The calculation equation is as follows:

$$H = \frac{\delta_G - \delta_P}{K} \times 100 + h \quad (1)$$

where H is the elevation of the recharge area, m; h is the elevation of the sampling point, m; δ_G is the $\delta^{18}O$ value of the geothermal spring; δ_P is the $\delta^{18}O$ value of atmospheric precipitation; and K is the $\delta^{18}O$ elevation gradient of atmospheric precipitation (δ/100 m). The gradient value of $\delta^{18}O$ is determined as follows: four typical cold springs were selected along the Zengjiuqu from upstream to downstream, and the $\delta^{18}O$ was obtained by fitting the $\delta^{18}O$ to the outcrop elevation of the spring. The curve is $\delta^{18}O$ = −0.0037*H-

TABLE 4 Recharge elevation of geothermal springs.

No.	Name	Isotopic results		Exposure elevation/m	Recharge elevation/m
		$\delta^{18}O$/‰	$\delta^{2}H$/‰		
1	Kanai geothermal spring	−19.86	−156.3	3933	5247
2	Waka geothermal spring	−19.71	−154.8	3920	5193
3	Cuoba geothermal spring	−19.46	−150.8	3988	5193
4	Luobusa geothermal spring	−11.96	−129.5	3568	2746
5	Zhenbucuo lake	−15.00	−121.6	4643	—

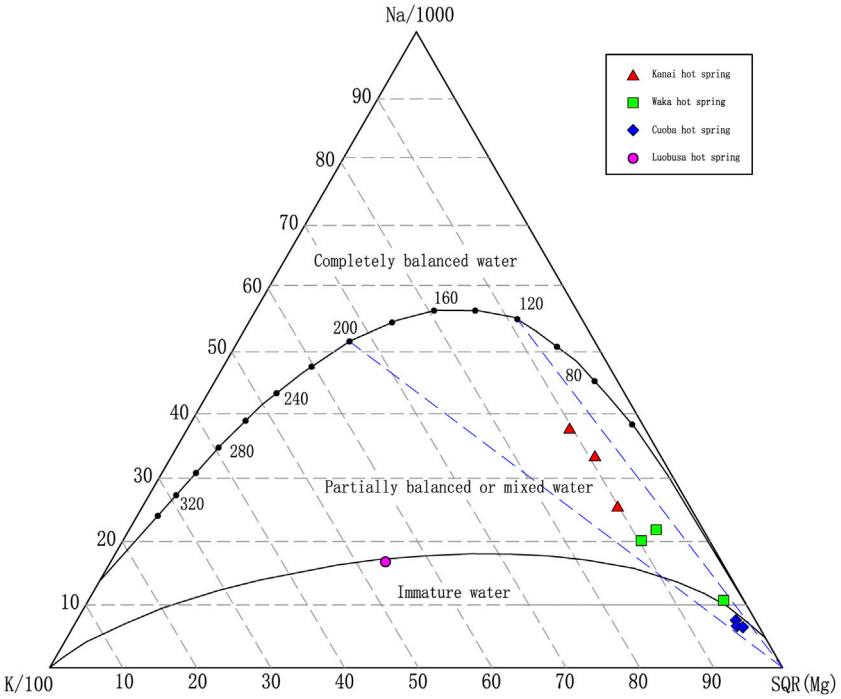

FIGURE 6
Na-K-Mg triangle diagram of geothermal waters.

107.98, R^2 = 0.9473, and the height gradient obtained from the fit is 0.37‰/100 m, which is in good agreement with the height gradient of 0.31‰/100 m in Tibetan area. The elevation reference value is determined as follows: The lake water is used as the elevation reference point, and its $\delta^{18}O$ = −15.0‰. The calculation results of the recharge elevation of each geothermal spring are shown in Table 4, and the results show that the recharge elevation of the geothermal water system in the Woka graben basin is 5193–5247 m, which is consistent with the elevation of the alpine basin where the regionally distributed snow mountains are located.

Reservoir temperature

The temperature of geothermal springs, as natural outcrops of geothermal water systems, is often low because of the mixing of shallow groundwater or surface water and cannot actually represent the temperature of the geothermal reservoir (Zhang, Xu, 2018; Li et al., 2020; Chang et al., 2021). Therefore, quantitative geochemical geothermometers such as SiO_2 and cation geothermometers are usually used to calculate the reservoir temperature (Fournier, 1977; Truesdell and Fournier, 1977; Fournier, 1979). As seen in Figure 6, the Kanai geothermal springs and the Woka geothermal springs all fall in the partially

TABLE 5 Relationship of water temperature, enthalpy, and SiO_2 concentration.

t/°C	S/4.1868J/g	ρc_{SiO2}/mg·L^{-1}
50	50.0	13.5
75	75.0	26.6
100	100.1	48.0
125	125.1	80.0
150	151.0	125.0
175	177.0	185.0
200	203.6	265.0
225	230.9	365.0
250	259.2	486.0
275	289.0	614.0
300	321.0	692.0

equilibrated zone or mixed water zone, and the Cuoba geothermal springs and the Luobosha geothermal springs fall in the immature water zone, indicating that the water–rock interaction in the geothermal water system of the Woka fault rift basin has not reached to complete equilibrium, or the geothermal water is mixed with a large proportion of cold water in a nonequilibrium state. Hence, the cation geothermometer has limitations in estimating the temperature of the reservoir. In this study, the SiO_2 geothermometer is selected for the calculation of the geothermal reservoir. The geothermal reservoir temperatures range from 95.22°C to 121.66°C (no steam loss) and 96.85°C–119.57°C (maximum steam loss), respectively, measured using the SiO_2 geothermometer. From the Na-K-Mg equilibrium diagram (Figure 6), it can be seen that the four outcrops of the Woka geothermal spring all fall between the 120°C and 200°C isotherms. In addition, the estimated reservoir temperatures based on the SiO_2 geothermometer are all lower than this range, indicating that the geothermal water in the basin is mixed by the shallow fractured cold water or surface water in the process of gushing out of the surface.

The above analysis shows that the geothermal springs in the Woka basin have the characteristics of mixing with shallow cold water, and a mixing model can be established to estimate the initial geothermal reservoir temperature in the deep position. The mixing model equation is as follows:

$$S_c X_1 + S_h (1 - X_1) = S_s \quad (2)$$

$$\rho c_{SiO2} X_2 + \rho h_{SiO2} X_2 (1 - X_2) = \rho S_{SiO2} \quad (3)$$

where S_c is the enthalpy of cold water (J/g); S_s is the final enthalpy of spring water (J/g, the enthalpy of saturated water below 100°C is equal to the number of the temperature of water in degree Celsius; above 100°C, the relationship between temperature and enthalpy of saturated water can be found in Table 5); S_h is the initial enthalpy of geothermal water (J/g); $\rho cSiO_2$ is the mass concentration of SiO_2 of cold water (mg/L); $\rho sSiO_2$ is the mass concentration of SiO_2 of spring water (mg/L); $\rho hSiO_2$ is the initial mass concentration of SiO_2 of geothermal water (mg/L); and X is the mixing ratio of cold water.

According to the above equation, the cold water temperature is taken as the local average annual temperature of 8.2°C in Woka, and the cold water SiO_2 content is taken as the average value of cold springs in the basin. The initial temperature of geothermal water is assumed to be equal to 75°C–300°C, and the corresponding enthalpy values can be found in Table 6. The temperature at the mouth of the spring and the SiO_2 content were based on the measured values. The enthalpy and the mass concentration of SiO_2 at each temperature are substituted into Eqs 1, 2, respectively, to find the X_1 and X_2 values at different temperatures and plot the curve of X and geothermal water temperature at different temperatures (Figure 6), and the intersection point of X_1 and X_2 curves is the calculated reservoir temperature value.

Figure 7 shows that the reservoir temperature of Kanai geothermal spring is 200°C, and the proportion of cold water mixing is 77%; the reservoir temperature of Woka geothermal spring is 175°C, and the proportion of cold water mixing is 73%; the reservoir temperature of Amaka geothermal spring is 175°C, and the proportion of cold water mixing is 83%; thus, it can be seen that the underground geothermal water system of Woka rift basin is a high-temperature geothermal water system, but it is strongly affected by the mixing of cold water on the surface. The estimated reservoir temperature based on the mixing model is basically consistent with the reservoir temperature range on the Na-K-Mg equilibrium diagram, which can reflect the reservoir temperature value of the subsurface geothermal water system in the Woka graben basin more realistically.

Genetic mechanism

Heat source

According to previous research on high-temperature geothermal systems in Tibet, the heat source of Tibetan geothermal heat is mostly the contribution of the local melt layer in the crust, which is characterized by high conductivity and low gravity anomalies (Zhang, Tan, 2015). The melt bodies are mostly arranged in a string of beads and form extensional faults and fracture zones with linear spreading characteristics on the surface. In addition, they gradually form a fault valley system characterized by a string of bead-like fracture basins in the later geological history, which often becomes the dominant site for underground geothermal water and nurtures many geothermal fields such as Nimu, Yangbajing, and Gulu. Combined with the hydrogeochemical characteristics of the geothermal springs exposed in the Woka graben, it is believed that there is a deep local melt in the Woka graben,

TABLE 6 Reservoir temperature of geothermal springs.

Spring name	T/°C	No steam loss	Max steam loss
		$t = \frac{1309}{5.19 - logSiO_2} - 273.15$	$t = \frac{1522}{5.75 - logSiO_2} - 273.15$
Kanai geothermal spring	51.96	121.66	119.57
Waka geothermal spring	52.65	112.44	111.70
Cuoba geothermal spring	36.25	95.22	96.85
Luobusa geothermal spring	57.77	212.41	194.32

which provides a good heat source condition for the underground geothermal water system in the Woka graben basin.

Transport channel

The interlocking fracture system in the Woka basin provides storage space and transport channels for the formation of geothermal water. From the point of view of the development of the geothermal water system, the intersection of fractures in different directions is the dominant part of geothermal water storage, transportation, enrichment, and even discharge and is the area with intensive geothermal water activity. The main heat control structure of the Woka geothermal area can be divided into the northern Regan–Songduo fault zone, the central Mocun fault zone, and the southern Yarlung–Zangbo River tectonic zone. They are distributed in the E-W direction and cut by the N-S direction Cuona–Woka fault. These tectonic intersections constitute the favorable location of the geothermal water system. In particular, the intersection of NS-oriented faults and EW-oriented faults is not only a channel for geothermal water recharging but also a space for geothermal water transportation and storage. Hence, it is the most active part of the geothermal water system, and the existence of a low-resistance zone has a resistivity of less than 100 Ω m, which is approximately 300 m wide, along the geothermal spring outcrop zone of the Zengjiuqu River Valley.

Recharging source

The analysis of hydrogeochemical characteristics shows that the geothermal springs in the study area are mainly recharged by atmospheric precipitation and snow-melting water. The geothermal water is affected by water–rock action and cold water mixing in the circulation process, showing different types of water chemistry. The geothermal springs in the area are mixed with cold water in varying proportions from 73 to 83%. The hydrogen and oxygen isotopic characteristics of the geothermal springs show that the geothermal springs in the area are recharged at elevations from 5193 to 5247 m.

Reservoir affinity

Based on the hydrogeochemical characteristics of the geothermal springs and their reservoir characteristics, the reservoirs in the area can be divided into two types: Quaternary pore and bedrock fracture.

Quaternary pore sediment reservoir

According to the results of physical prospecting, the thickness of the fourth series loose cover layer of Zengjiuqu in the Woka area is 50–150 m. In addition, its lithology is sand and gravel, with a dense sand layer or geothermal water colloid layer as a cover layer locally. In the process of recharge and runoff, the geothermal water gushes out along the buried Woka fault developed in the basement of the riverbed or the boundary faults on both sides of the Woka rift basin. Then, geothermal water enters into the pore space of the Quaternary loose sediments with good permeability along the valley of Zengjiuqu, forming a good Quaternary pore sediment reservoir.

The outcrop of geothermal water in this geothermal reservoir is mainly a warm water swamp. In addition, the outcrop along Zengjiuqu is wide. The closer distance to the surface water is, the more obvious the mixing effect is, and the temperature is lower. However, the borehole can reveal underground geothermal water with a higher temperature than the natural outcrop geothermal spring.

Bedrock fracture type reservoir

This reservoir is mainly distributed in the bedrock on both sides of Zengjiuqu, and its aquifer is composed of Cretaceous–Paleocene granite intrusive rocks, which are influenced by active faults, and the tectonic fissures are developed, with rich water reserve. The development of tectonic fissures is not only an advantageous channel for geothermal water transportation but also an excellent space for geothermal water storage. Most of the geothermal springs flow along the fissures in granite, which is the main reservoir of geothermal water in the area.

Conceptual model for geothermal system in the Woka graben

Because of the continuous and strong plate collision activities of the Eurasian plate, intensive and frequent structural deformation has been formed on the Tibetan Plateau. It creates a deep melt-type magma source area in

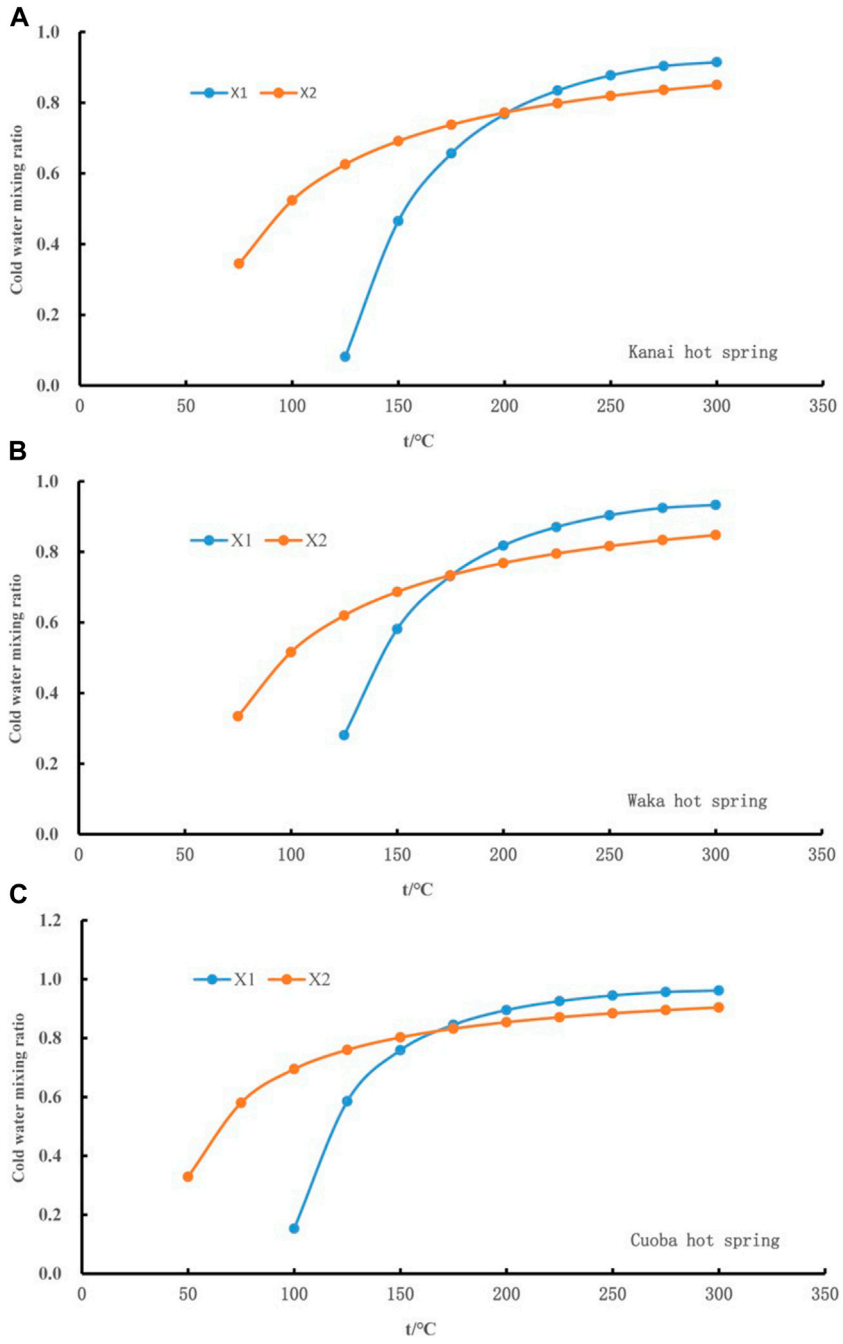

FIGURE 7
Relations between fraction of cold water and temperature in the mixing model.

the lower crust and a local low-velocity melt layer in the middle and forms shallow intrusive magma capsules and local banded melt bodies at different depths within a certain depth in the upper crust, providing the necessary heat source for the formation of the underground geothermal water system on the Tibetan Plateau. Therefore, the Tibetan Plateau geothermal resources are mostly uplifted mountain convection type. The conceptual model of the subsurface geothermal water system within the Woka graben basin was established by synthesizing the research results of many geothermal fields in the Tibetan region, such as Yangpaijing and Nimu-Naqu geothermal fields (Figure 8).

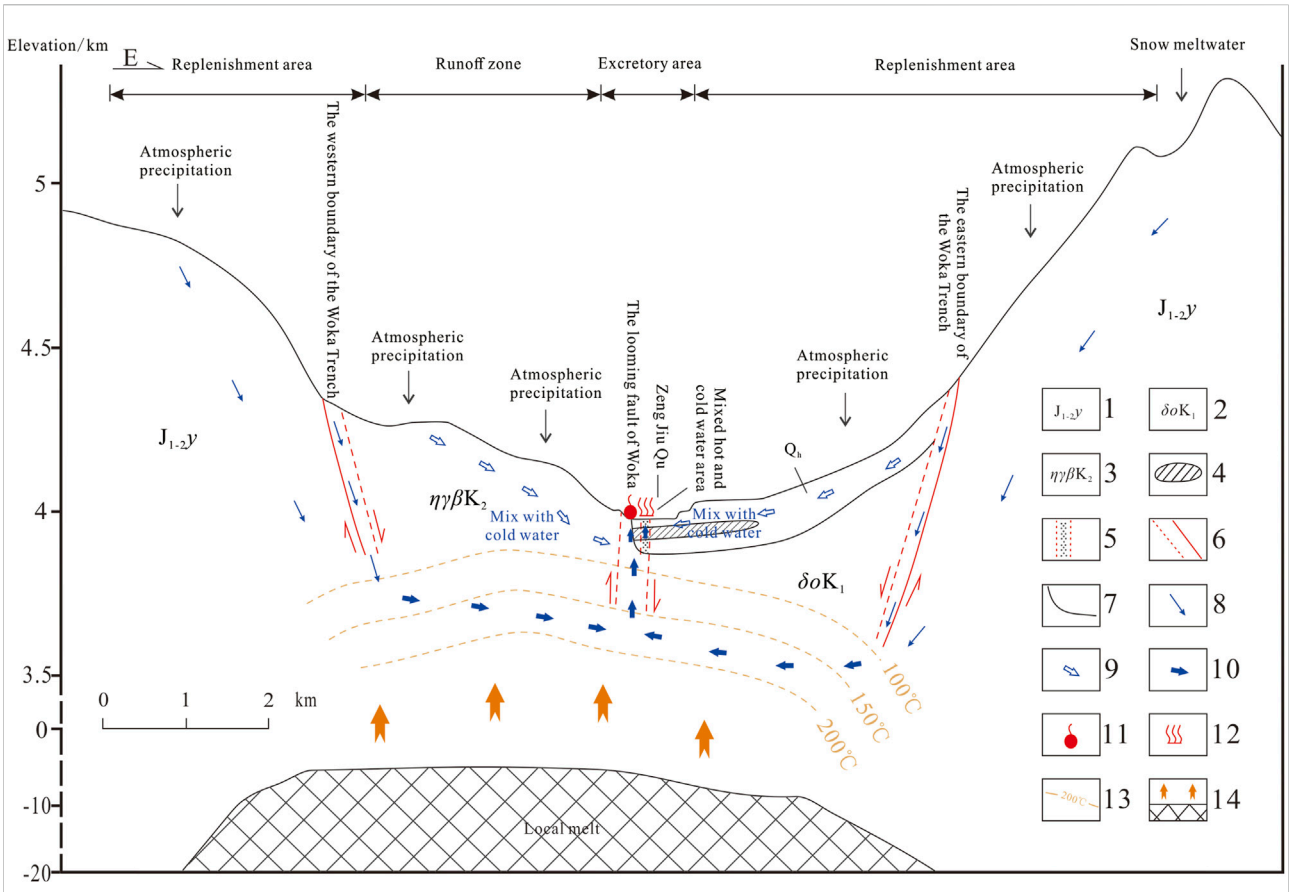

FIGURE 8
Genetic model of geothermal waters in the Woka Graben basin. 1-Middle to Lower Jurassic Yeba formation; 2-Lower Cretaceous quartz diorite; 3-Middle Cretaceous monzogranite;4-Tight sand cover; 5-Channel of Quaternary thermal reservoir; 6-Measured or inferred fault; 7-Geological boundary; 8-Cold water and transport direction; 9-Mixed cold water and its migration direction; 10-Geothermal water and flow direction; 11-Geothermal spring; 12-Warm water swamp; 13-Inferred temperature contour; 14-Heat source.

The atmospheric precipitation and alpine ice and snow melt water on both sides of the Woka graben basin are the main recharge sources of geothermal water, and the cold water receiving the recharge keeps seeping down along the fractures developed by the tectonic activity. In addition, cold water is heated by the local strip melt at a certain depth to provide a heat source and thus forms geothermal water involved with deep gas components. Then, geothermal water begins to flow upward, controlled by the fault-controlled bedrock fracture type reservoir. During the ascent of geothermal water along the river valley or the basin boundary fractures, its temperature decreases because of the mixing of the shallow cold water. In Zengjiuqu River valley, geothermal water enters into the pore aquifer of the fourth system loose rock type with good permeability along the bedrock fracture reservoir. In addition, the dense sand layer or geothermal water cementation layer is used as the cover layer, forming the Quaternary pore type shallow reservoir, which is mixed with the surface water during the rising of geothermal water and forms a warm water swamp along the riverbed.

The effect of high-temperature geothermal water on underground construction

The Woka graben is adjacent to Mochukongka Qu in the north and reaches the valley of Yarlung Tsangpo River in the south, which is an essential place for the Sichuan–Tibet railway line. Because of the construction of the Lhasa–Linzhi railway, many major projects such as hydropower and road construction are further planned in the area. According to the above analysis, the geological structure of Woka graben is complex, with active fracture development and strong hydrothermal activity, and its deep reservoir temperature can reach more than 120°C. Hence, it belongs to the high- and medium-temperature geothermal system. Engineering construction will be affected by the enrichment of geothermal resources.

As for the engineering thermal damage, the water temperature of the surface outcrop in the Woka rift valley is 36.25°C–57.77°C, and the calculated reservoir temperature is 97.86°C–125.56°C. The water temperature in the deep or good geothermal channels will be even higher. After the project exposure, there will be a large flow of high-temperature geothermal water caused by the surge water disaster; the sulfate content of geothermal water in the graben is 94.4–147 mg/L, and toxic and harmful gases such as H_2S will be escaped after the project exposure. Therefore, the construction of the project in the geothermal development area of the rift valley will pose a great threat to the safety of construction workers because of the high-temperature geothermal water and harmful gases, leading to a significant increase in project costs.

As for the corrosiveness of the project, the pH value of the geothermal water in the rift valley is 6.71–8.25, the HCO_3^- content is 31–214 mg/L, the Mg^{2+} content is 0.026–7.85 mg/L, and the SO_4^{2-} content is 94.4–147 mg/L, which is not corrosive to the project. However, the Cl^- ion content of the Luobusa geothermal spring is 4060 mg/L, which is more than 1000 mg/L. It is a corrosive hazard to the tunneling equipment as well as the tunneling facilities, which must be considered in tunnel construction. Therefore, for major construction projects in the Woka graben, a detailed investigation should be conducted to avoid the geothermal water channel or to divert the geothermal water and reasonably arrange the construction sequence to overcome the problem.

Conclusion

(1) The geothermal water system in the Woka graben belongs to the medium- to high-temperature geothermal system, and the geothermal heat shows a belt-like distribution along the Woka semiburied fracture. The geothermal water is medium alkaline water with a TDS concentration of 150.8–744 mg/L. The hydrochemical types are mainly SO_4-Na type, SO_4-Cl-Na type, and HCO_3-SO_4-Na type.

(2) The hydrogeochemical characteristics show that the Woka geothermal water system has the characteristics of atmospheric precipitation recharge and shallow circulating groundwater and is subject to the mixing effect of fracture diving or surface water. In addition, the geothermal water is in the range of partial equilibrium or mixed water and immature water on the Na-K-Mg equilibrium diagram.

(3) The reservoir temperatures range from 97.86°C to 125.56°C, estimated using a silica geothermometer. The geothermal water was subject to the mixing of shallow fissure cold water or surface water. By establishing the reservoir temperature mixing model, the initial reservoir temperature of geothermal water and the proportion of mixed cold water are determined. The temperature range of shallow and deep geothermal reservoirs is from 96.85°C to 119.57°C and from 120°C to 200°C, respectively, and the proportion of mixed cold water is 73–83%.

(4) Based on the isotope elevation effect characteristics, the recharge elevations of the geothermal water system in the Woka graben basin are from 5193 to 5247 m, mainly recharged by atmospheric rainfall and alpine snow-melting water, and the geothermal water comes from the release of mantle-sourced CO_2 from deep regional faults.

(5) Some geothermal waters possess high Cl^- concentrations, leading to the corrosiveness of the project. For major construction projects in the Woka graben, a detailed investigation should be conducted to avoid the geothermal water channel or to divert the geothermal water and reasonably arrange the construction sequence to overcome the problem.

Data availability statement

The original contributions presented in the study are included in the article/Supplementary Material; further inquiries can be directed to the corresponding author.

Author contributions

WZ: Investigation, data curation, and writing—original draft. SW: Data curation and methodology. MX: Writing—review and editing and conceptualization.

Conflict of interest

SW is employed by the Sichuan Institute of Geological Engineering Investigation Group Co., Ltd.

The remaining authors declare that the research was conducted in the absence of any commercial or financial relationships that could be construed as a potential conflict of interest. The reviewer YL declared a shared affiliation with the author WZ to the handling editor at the time of review.

Publisher's note

Supplementary material

The Supplementary Material for this article can be found online at: https://www.frontiersin.org/articles/10.3389/feart.2022.895884/full#supplementary-material

References

Cao, H-W., Li, G-M., Zhang, R-Q., Zhang, Y-H., Zhang, L-K., Dai, Z-W., et al. (2021). Genesis of the Cuonadong tin polymetallic deposit in the tethyan himalaya: evidence from geology, geochronology, fluid inclusions and multiple isotopes. *Gondwana Res.* 92, 72–101. doi:10.1016/j.gr.2020.12.020

Cao, H-W., Li, G-M., Zhang, Z., Zhang, L-K., Dong, S-L., Xia, X-B., et al. (2020). Miocene Sn polymetallic mineralization in the tethyan himalaya, southeastern tibet: a case study of the cuonadong deposit. *Ore Geol. Rev.* 119, 103403. doi:10.1016/j.oregeorev.2020.103403

Cao, H-W., Zhang, Y-H., Santosh, M., Li, G-M., Hollis, S. P., Zhang, L-K., et al. (2019). Petrogenesis and metallogenic implications of cretaceous magmatism in central lhasa, tibetan plateau: a case study from the lunggar Fe skarn deposit and perspective review. *Geol. J.* 54, 2323–2346. doi:10.1002/gj.3299

Chang, X-W., Xu, M., Jiang, L-W., Li, X., and Zhang, Y-H. (2021). Hydrogeochemical characteristics and formation of low-temperature geothermal waters in mangbang-longling area of western yunnan, China. *J. Chem.* 2021, 1–13. doi:10.1155/2021/5527354

Elenga, H. I., Tan, H., Su, J., and Yang, J. (2021). Origin of the enrichment of B and alkali metal elements in the geothermal water in the Tibetan Plateau: Evidence from B and Sr isotopes. *Geochemistry* 81, 125797. doi:10.1016/j.chemer.2021.125797

Fournier, R. (1977). Chemical geothermometers and mixing models for geothermal systems. *Geothermics* 5, 41–50. doi:10.1016/0375-6505(77)90007-4

Fournier, R. O. (1979). Geochemical and hydrologic considerations and the use of enthalpy-chloride diagrams in the prediction of underground conditions in hot-spring systems. *J. Volcanol. Geotherm. Res.* 5, 1–16. doi:10.1016/0377-0273(79)90029-5

Guo, Q. (2012). Hydrogeochemistry of high-temperature geothermal systems in China: a review. *Appl. Geochem.* 27, 1887–1898. doi:10.1016/j.apgeochem.2012.07.006

Jiang, Z., Xu, T., Owen, D. D. R., Jia, X., Feng, B., Zhang, Y., et al. (2018). Geothermal fluid circulation in the Guide Basin of the northeastern tibetan Pplateau: isotopic analysis and numerical modeling. *Geothermics* 71, 234–244. doi:10.1016/j.geothermics.2017.10.007

Klemperer, S. L., Zhao, P., Whyte, C. J., Darrah, T. H., Crossey, L. J., Karlstrom, K. E., et al. (2022). Limited underthrusting of India below Tibet: $^{(3)}$He/$^{(4)}$He analysis of thermal springs locates the mantle suture in continental collision. *Proc. Natl. Acad. Sci. U. S. A.* 119, e2113877119. doi:10.1073/pnas.2113877119

Kong, Y., Pang, Z., Shao, H., Hu, S., and Kolditz, O. (2014). Recent studies on hydrothermal systems in China: a review. *Geotherm. Energy* 2, 19. doi:10.1186/s40517-014-0019-8

Li, X., Huang, X., Liao, X., and Zhang, Y. (2020). Hydrogeochemical characteristics and conceptual model of the geothermal waters in the xianshuihe fault zone, southwestern china. *Int. J. Environ. Res. Public Health* 17, 500. doi:10.3390/ijerph17020500

Li, X., Qi, J., Yi, L., Xu, M., Zhang, X., Zhang, Q., et al. (2021). Hydrochemical characteristics and evolution of geothermal waters in the eastern himalayan syntaxis geothermal field, southern tibet. *Geothermics* 97, 102233. doi:10.1016/j.geothermics.2021.102233

Liao, Z. (2018). Hot springs in southwestern China. *Therm. Springs Geotherm. Energy Qinghai-Tibetan Plateau Surroundings* chapter 6, 79–163. doi:10.1007/978-981-10-3485-5_6

Tan, H., Su, J., Xu, P., Dong, T., and Elenga, H. I. (2018). Enrichment mechanism of Li, B and K in the geothermal water and associated deposits from the kawu area of the tibetan plateau: constraints from geochemical experimental data. *Appl. Geochem.* 93, 60–68. doi:10.1016/j.apgeochem.2018.04.001

Tian, J., Pang, Z., Liao, D., and Zhou, X. (2021). Fluid geochemistry and its implications on the role of deep faults in the genesis of high temperature systems in the eastern edge of the Qinghai Tibet Plateau. *Appl. Geochem.* 131, 105036. doi:10.1016/j.apgeochem.2021.105036

Truesdell, A., and Fournier, R. (1977). Procedure for estimating the temperature of a hot-water component in a mixed water by using a plot of dissolved silica versus enthalpy. *USGS J. Res.* 5, 49–52.

Wang, P., Chen, X., Shen, L., Wu, K., Huang, M., Xiao, Q., et al. (2016). Geochemical features of the geothermal fluids from the mapamyum non-volcanic geothermal system (Western Tibet, China). *J. Volcanol. Geotherm. Res.* 320, 29–39. doi:10.1016/j.jvolgeores.2016.04.002

Wang, Y., Gu, H., Li, D., Lyu, M., Lu, L., Zuo, Y., et al. (2021). Hydrochemical characteristics and Genesis analysis of geothermal fluid in the zhaxikang geothermal field in cuona county, southern tibet. *Environ. Earth Sci.* 80, 415. doi:10.1007/s12665-021-09577-8

Wang, Y., Li, L., Wen, H., and Hao, Y. (2022). Geochemical evidence for the nonexistence of supercritical geothermal fluids at the yangbajing geothermal field, southern tibet. *J. Hydrology* 604, 127243. doi:10.1016/j.jhydrol.2021.127243

Wang, Y., Zheng, C., and Ma, R. (2018). Review: safe and sustainable groundwater supply in China. *Hydrogeol. J.* 26, 1301–1324. doi:10.1007/s10040-018-1795-1

Zhang, W., Tan, H., Zhang, Y., Wei, H., and Dong, T. (2015). Boron geochemistry from some typical tibetan hydrothermal systems: origin and isotopic fractionation. *Appl. Geochem.* 63, 436–445. doi:10.1016/j.apgeochem.2015.10.006

Zhang, X., and Hu, Q. (2018). Development of geothermal resources in China: a review. *J. Earth Sci.* 29, 452–467. doi:10.1007/s12583-018-0838-9

Zhang, Y., Xu, M., Li, X., Qi, J., Zhang, Q., Guo, J., et al. (2018). Hydrochemical characteristics and multivariate statistical analysis of natural water system: a case study in kangding county, southwestern China. *Water* 10, 80. doi:10.3390/w10010080

Zhang, Y., Cao, H., Hollis, S., Tang, L., Xu, M., Jiang, J., et al. (2019a). Geochronology, geochemistry and Sr-Nd-Pb-Hf isotopes of the early paleogene gabbro and granite from central lhasa, southern tibet: petrogenesis and tectonic implications. *Int. Geol. Rev.* 61, 868–894. doi:10.1080/00206814.2018.1476187

Zhang, Y., Wang, Y., Wang, W., Liu, J., and Yuan, L. (2019b). Zircon U-Pb-Hf isotopes and mineral chemistry of early cretaceous granodiorite in the lunggar iron deposit in central Lhasa, Tibet Y, China. *J. Central South Univ.* 26, 3457–3469. doi:10.1007/s11771-019-4266-5

Zhang, Y., Yao, R., Wang, Y., Duo, J., and Cao, H. (2022). Zircon U-Pb and sericite Ar-Ar geochronology, geochemistry and S-Pb-Hf isotopes of the Zebuxia Pb-Zn deposit, Tibet, southwestern China. *Ore Geol. Rev.* 148, 104999. doi:10.1016/j.oregeorev.2022.104999